Available online at www.sciencedirect.com
ScienceDirect
Journal of the European Ceramic Society 27 (2007) 109–114
www.elsevier.com/locate/jeurceramsoc

Microstructural and optical features of a Eu-monazite

T. Hernández *, P. Martín

CIEMAT, Materiales Para Fusión, Avda. Complutense 22, 28040 Madrid, Spain

Received 3 February 2006; received in revised form 25 April 2006; accepted 6 May 2006
Available online 16 June 2006

Abstract

The obtention of europium-phosphate nanoparticles by the precipitation method and its thermal evolution to become ceramics materials is presented. The monazite structure was obtained from the rabdophane phase after firing at 1000 °C during several hours. The powder characteristics made easy the pressing and sintering processes and it was possible to obtain high density bodies (relative density > 97%) at only 1200 °C. The fluorescence spectra and the lifetimes were investigated as a function of the heating temperature, as well, the microstructure and the residual glassy phase. It was found that higher sintering temperatures (>1500 °C) resulted in lower fluorescence emission than lower temperatures (maximum at 1200 °C) as consequence of the microstructure detrimental. The gamma irradiation up to the dose of 18 kGys did not produce any appreciable effect in the optical properties; however, the sintering temperature modified the optical absorption in the UV range.

Keywords: Eu-monazite; Microstructure; Photoluminescence; $EuPO_4$

1. Intoduction

Rare-earth phosphate monazite-type has a variety of potentially beneficial properties, including very low solubility in water, high thermal stability, high index of refraction and optical properties suitable for laser applications.[1,2] Other functions concern the ability of the ceramic phosphate-containing matrices for the immobilization of actinides radionuclides, that is important for the containment of waste generated by the nuclear fuel cycle.[3] On the other hand, the optical properties of polycrystalline phosphates made by conventional techniques are generally poor due to large grain size and residual porosity, and effective sintering requires very high temperatures and pressures. Since optical properties are so sensitive to atomic structure, this has received considerable attention[4,5] as well the phase equilibrium in the systems Ln_2O_3–P_2O_5–H_2O.[6] There have been few systematic studies on synthesis and sintering of monazite-type $EuPO_4$. Several authors have reported the synthesis of rare earth phosphate compounds via different methods, such sol–gel,[7] high temperature solid reaction,[8] crystallization from boiling phosphoric acid solution,[9] or direct evaporation.[10] This paper discusses the characteristics of the nanopowders obtained by the precipitation technique and the ratio between the optical properties and the microstructural changes as consequence of the heating treatment and the γ-irradiation.

2. Experimental

2.1. Powder synthesis and characterization methods

The synthesis, carried out at room temperature, was based on reacting H_3PO_4 (0.4 M) (98%) with Europium nitrate solutions in equal molar ratio. A stoichiometric amount of $Eu(NO_3)_3$ dropwise to the H_3PO_4 solution while stirring to obtain a white precipitate that was dried at 120 °C. The chemical analysis of the phosphorous and europium in the precipitate was carried out in a multielemental ICP spectrometer (Thermo Jarrell Ash, mod. Iris). The P:Eu ratio was 1.09, slightly than the stoichiometric value of 1.

The hydrodynamic phosphate nanoparticles size in the precipitate was measured at room temperature by photon correlation spectroscopy (PCS), using an argon laser particle size analyzer MALVERN 4700 model of 500 mW output power emitting at 514 nm wavelength.

The crystalline phases, obtained for each heating treatment, were analysed by X-ray diffraction (XRD, Philips diffractometer X-Pert-MPD) with CuKα radiation and Si monochromator.

* Corresponding author. Tel.: +34 91 346 6770; fax: +34 91 346 6005.
E-mail address: teresa.hernandez@ciemat.es (T. Hernández).

0955-2219/$ – see front matter © 2006 Published by Elsevier Ltd.
doi:10.1016/j.jeurceramsoc.2006.05.091

Thermogravimetry (TG) and differential thermal analysis (DTA) tests were performed in a SEIKO TG/DTA 6300 equipment. The samples were heated from room temperature to 1200 °C at 10 °C/min

The calcined powders and the microstructure of mirror-like polished thermal etched sintered samples were studied by a scanning electron microscope (SEM, JEOL JSM 6400 at 20 kV and ADX LINK INCA).

The photoluminescence emission and excitation spectra were measured at room temperature with a Cary Eclipse luminescence spectrometer (equipped with a Hamamatsu R3896 photomultiplier) sensitive in the range 200–900 nm. The excitation was produced with a xenon flash lamp (~2 μs pulse-width) and fluorescence spectra were recorded 0, 1 ms after the flash and with 5 ms gate time. The bandwidth excitation and emission was 5 nm. Suitable spectral filters were used to prevent second order diffraction. The measurements of fluorescence dynamics were carried out 0, 1 ms after the flash of the xenon lamp and with 3 μs gate time.

Absorption measurements were performed with a Cary 5E spectrometer in the UV–vis-NIR range (200–3000 nm).

Gamma irradiations were performed in the CIEMAT ^{60}Co pool facility (NAYADE), that permits a controlled atmosphere at a typical dose rate around 10 Gy/s.

3. Results and discussion

3.1. Characterization of powder

The Eu-phosphate obtained by precipitation exhibits a particle size of 135 ± 4 nm. Such data correspond to the mean and its standard deviation and were obtained from different PCS measurements as can be seen in Fig. 1. Such particles are elongated as large hexagonal bars and are weakly agglomerated, as shown in Fig. 2a and b. They change to spherical particles when the temperature is increased and are transformed into monazite-type (Fig. 2c).

The Fig. 3 shows the temperature programmed XRD patterns of $EuPO_4$ powders. The broad peak at room temperature indicates that rhabdophane-type powders were formed of small

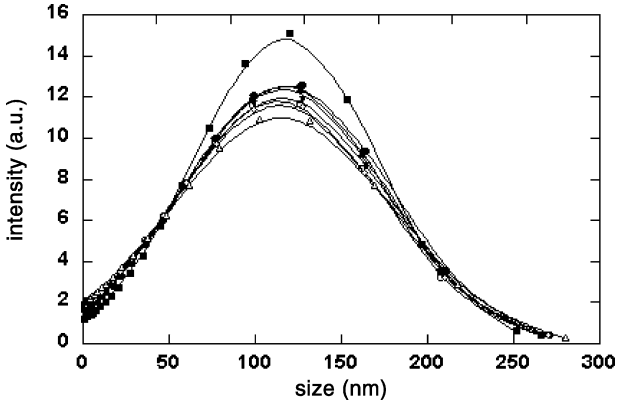

Fig. 1. Hydrodynamic size distribution in the precipitate suspension measured by PCS.

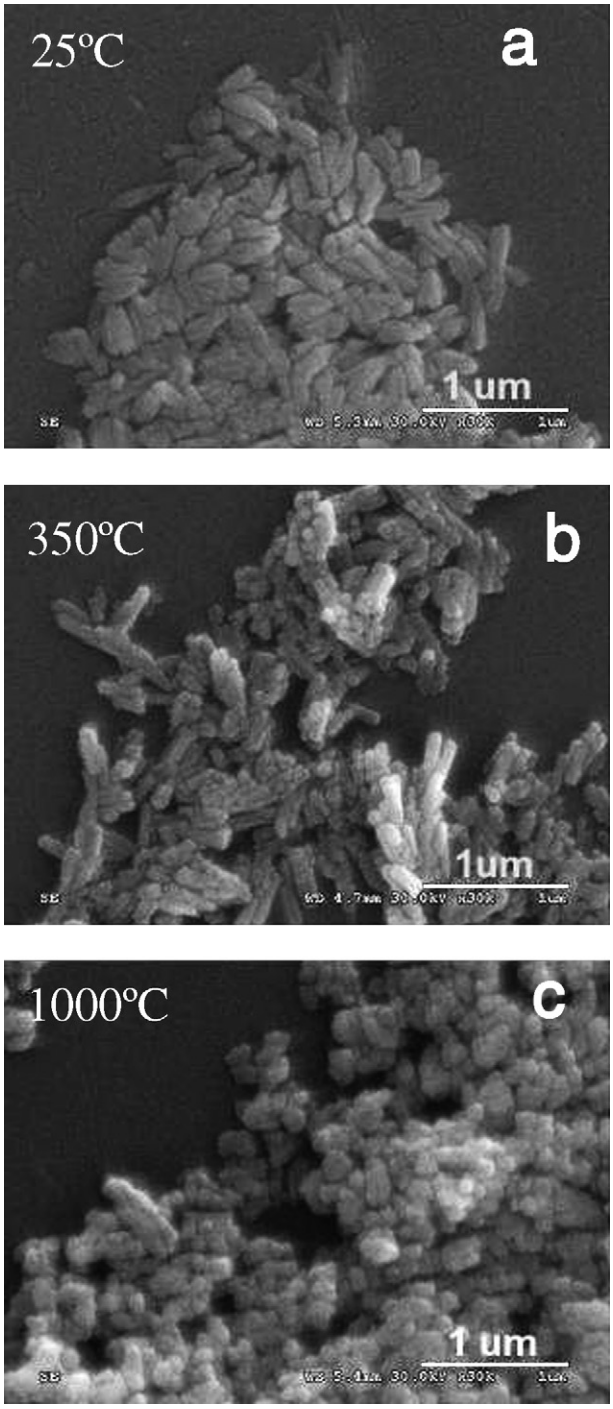

Fig. 2. Particles morphology obtained from precipitation a) hydrated $EuPO_4{\cdot}nH_2O$, b) $EuPO_4{\cdot}nH_2O$ rhabdophane-type at 350 °C and C) $EuPO_4$ monazite-type obtained at 1000 °C.

crystallites. The same phase is also detected at 350 °C, however at 1000 °C the rhabdophane phase was disappeared to transform into monazite, which has monoclinic structure. X-ray peak intensities of monazite increased as heating temperature were increased and no other phases were detected in the heated specimens up to 1600 °C

Decomposition of the precursor and formation of europium phosphate was followed by thermal analysis data provided in

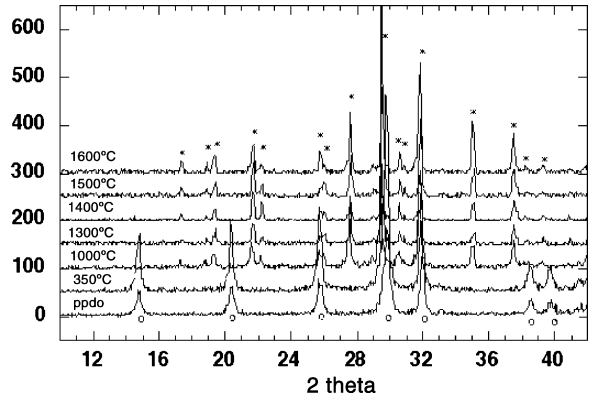

Fig. 3. Phase evolution with temperature from the precipitation synthesis at room temperature to sintering temperatures of 1600 °C. Open circles: rhadophane, asterisks: monazite.

Fig. 4. The TGA curve shows three-step decomposition of the europium phosphate precursor. The 66.2% weight loss was observed below 130 °C. A narrow and sharp endothermic peak was found around 90 °C which is related with the removal of absorbed water. The evolution of water of hydration of europium phosphate takes place at 150 and 250 °C. The weight loss measured during this second step corresponds to the hydration ratio n of the rhabdophane ($EuPO_4{\cdot}nH_2O$) about 0.47 moles. On the hypothesis of pure europium phosphate is obtained, no detectable weight change over 300 °C was expected to occur. However, it is possible to observe a soft exothermic peak at 830 °C. Some authors have confirmed that the irreversible rhabdophane-monazite transformation takes place once dehydration is completed and the transformation is accomplished by heating close to 800 °C.[11] The heat of such transformation increases with the atomic number, until those rare earths that for xenotime-structure hydrated phosphates are reached (Dy). In this case, such peak is very smooth but noticeable enough.

The P:Eu ratio was 1.09 in the calcined powders and so on, the possibility that EuP_2O_7 dehydrated or polytrioxophosphate were formed is quite low. Such crystalline phases would have to be detected by some additional peaks registered on the XRD diagram of the europium phosphate, or associated with extra peaks in the TG-DTA plots because they are produced and decomposed with evolution of oxygen gas and simultaneously strong exothermic and endothermic peaks at 600 and 873 °C[12] and 950 and 1250 °C[13], respectively.

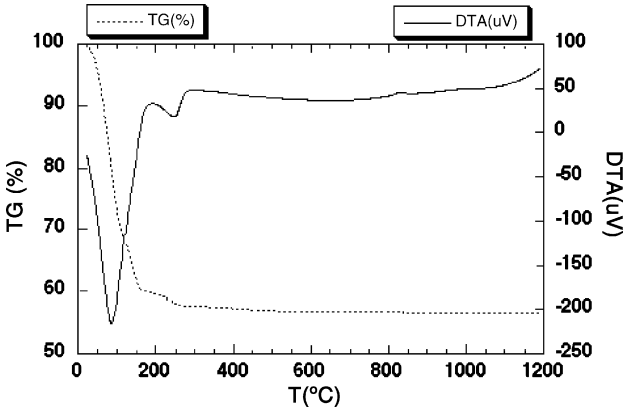

Fig. 4. Thermal analysis (DTA/TGA) graph of europium phosphate precursor.

3.2. Sintering and microstructure

The green density after isostatic pressing was over 50% which means that the aggregates formed during heating at 1000 °C to obtain the monazite phase were quite soft and could break when the press was applied, the rounded size of the powders made easy the packing. After sintering, the relative density for four hours soakings was always over 98% and did not depend on temperature from 1300 at 1600 °C. In this sintering temperature range the density was maintained constant, only at 1200 °C the density was slightly lower (97%).

The sintered bodies microstructures can be observed in Fig. 5. Since lower sintering temperatures (1200 °C) to the higher (1600 °C) the general features are similar. Mainly equiaxed grains of a broad size form such material. At 1200 °C the grains are ranged between 2 and 10 microns and grow up at 1600 °C to 10 and 30 microns. In addition to this usual coarsening size behaviour, two important facts can be observed. The first one is related with the second glassy phase rounding the monazite grains, such phase is more plentiful for the lower sintering temperatures and to be efficient the liquid phase must wet the solid. The apparition of the glass phase would lead to the existence of an endothermic DTA peak over 1200 °C, however, in our case temperature just reach to 1175 °C. The second one is that even at 1200 °C some sporadic abnormal large grains are formed coexisting with the equiaxed grain matrix (not showed in the figure). These grains can reach an enormous size of about 400 microns when temperature is increased to 1600 °C. Finally, to comment that at 1200 °C the porosity has not disappeared completely and some pores remain into the grains and the grain boundaries denoting that the grains coalescence and the sintering reaction are happening but are not yet finished while some glassy phase emerges at the grain boundaries and triple points as it is shown in Fig. 5C. The sintering is completely finalized at 1300 °C, as can be seen in the Fig. 5a, where only a minimal residual porosity is located at the triple junctions.

As it is known, it is difficult to prepare residual glass free $REPO_4$. An important determinant of the glass forming regions is the cation size, and the Eu^{3+} has a small valence-stable by bonding with $PO_4{}^{3+}$ tetrahedra. The light excess of $PO_4{}^{3+}$ is assumed to be adsorbed at the particle surfaces[14]; however, it is not sufficient to develop any of the crystalline phases as EuP_2O_7 or EuP_3O_9. In our material the P_2O_5 exceeds Eu and is segregated at the grain boundaries as glass, as can be seen in Fig. 5c. The P/Eu ratio is 1.09 as the elemental analysis demonstrates, and the calculated ratio P/O is 0.25. In such conditions the phosphate portion of the network glass is expected to be composed of shorter chains[15]. This fact seems decisive for the high densification during sintering at low temperatures. When the densification begins, the mobility of the short chains of the glassy phase can be important for moderate temperatures of 1200 °C and allow the complete densification at 1300 °C by promoting mechanisms that are effective in the densification of the material, specially the grain boundary diffusion. The flexibility of the structure is

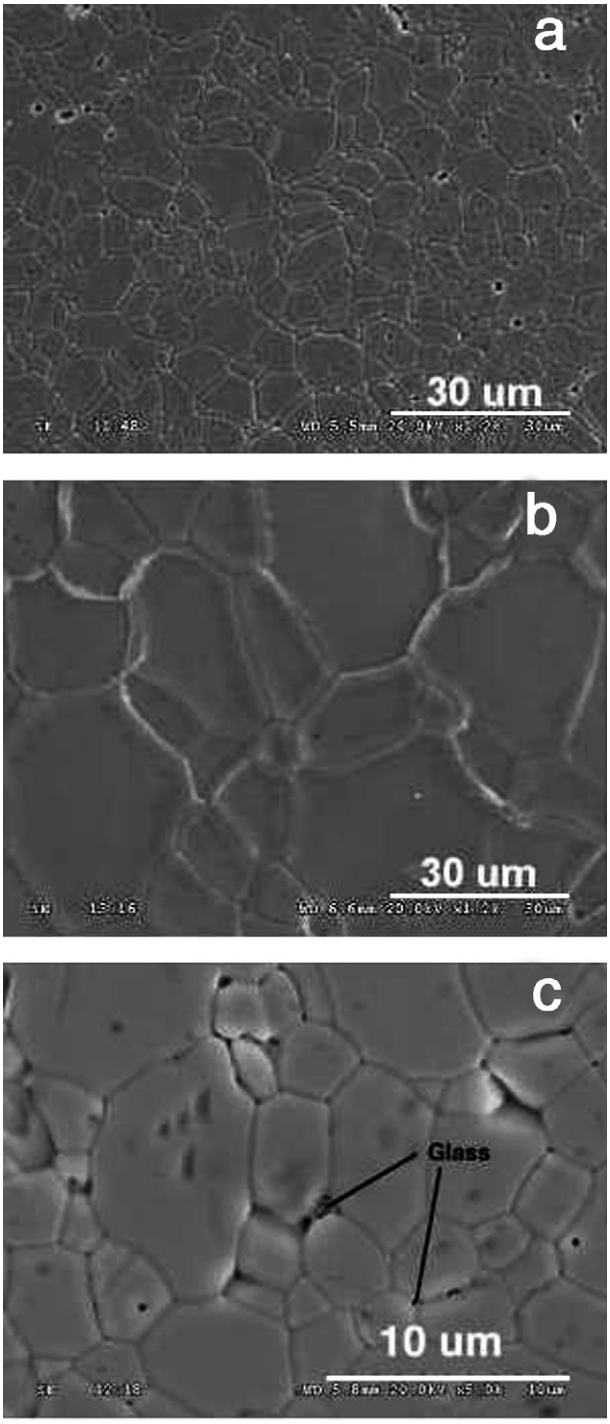

Fig. 5. Microstructure of the samples sintered at 1300 °C (a) and 1600 °C (b) for 4 h, (c) glassy phase at sintering temperature of 1200 °C.

a key factor for the formation of a disordered glass and determines the glass-forming ability of glass formation regions. This looks to be significant for europium/phosphate system and is agree with the short chains glass hypothesis. On the other hand, the crystallization of a glass is governed, to a large extent, by structural-chemical factors. The sequence of the formation of different crystalline phases along the crystallization path with an increase in temperature corresponds to the sequence of liberation of glass structure components, which is determined by

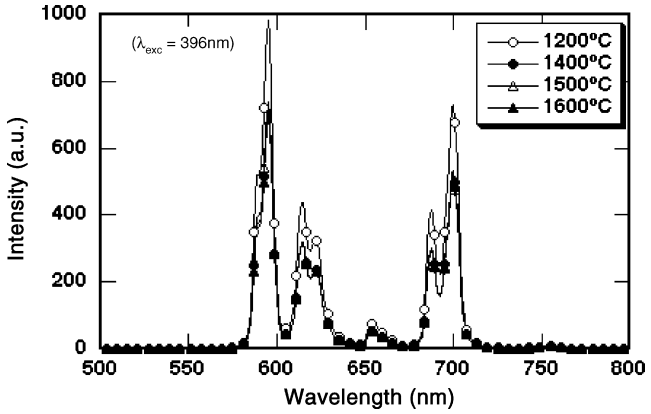

Fig. 6. Room temperature photoluminescence emission spectra of $EuPO_4$ under 396 nm excitation, sintering temperatures 1200, 1300, 1400, 1500, and 1600 °C.

the strength of chemical bonds and the flexibility of glass structure. This fact appears to be happening for the higher sintering temperatures, when the amount of glass is lower noticeable by SEM than for the inferior sintering temperatures.

3.3. Luminescence absorption and γ-irradiation

The fluorescence spectrum of $EuPO_4$ under UV excitation is due to the $4f \rightarrow 4f$ electronic transitions in Eu^{3+} between the lowest excited state $^5D_0$ and the ground state ^7F_J[16]. In Fig. 6 are displayed the emission spectra of $EuPO_4$ for samples sintered at temperatures from 1200 to 1600 °C, under 396 nm excitation at room temperature, (spectra present the characteristic peaks about 595 nm for $^5D_0 \rightarrow {}^7F_1$, 614 nm for $^5D_0 \rightarrow {}^7F_2$, 654 nm for $^5D_0 \rightarrow {}^7F_3$and 700 nm for $^5D_0 \rightarrow {}^7F_4$ transitions) as can be seen samples sintered at lower temperature shows higher intensity. In general, the forbidden electric-dipole transition $^5D_0 \rightarrow {}^7F_2$ (614 nm) of Eu^{3+} is expected to dominate in the emission spectrum if Eu^{3+} ions occupy asymmetric sites in the lattice[17] however in phosphates such as YPO_4[18] and $LaPO_4$[14] the magnetic dipole transition $^5D_0 \rightarrow {}^7F_1$ (595 nm) becomes stronger than the electric-dipole transition due to effects of phosphate groups in the host lattices. These transitions $^5D_0 \rightarrow {}^7F_1$ (595 nm) and $^5D_0 \rightarrow {}^7F_2$ (614 nm) are hypersensitive transitions and their intensity depends strongly on the chemical and structural environment inside the host matrix. No appreciable differences in the emission spectra were found under excitation from f-f transitions such as at 396 nm wavelength ($^7F_0 \rightarrow {}^5L_6$ transition) and exciting at 267 nm, this band is attributed to charge transfer between oxygen and europium.[19,20]

Fig. 7 shows the excitation spectra monitored at 595 nm wavelength Samples sintered at higher temperature presents lower intensity excitation at wavelengths around 267 nm. No appreciable differences in the excitation spectra were found monitoring at wavelength 615 and 700 nm. Lines observed at 320, 363, 383, 396, 416, 465, and 526 nm are associated with $f \rightarrow f$ transitions of Eu^{3+}.[21]

A luminescence study of single-crystal $EuPO_4$ at high pressure was made by G. Chen et al.[22] They found that the luminescence spectrum and the luminescence lifetime are good monitors to study the effect of pressure on the crystal structure. Our $EuPO_4$

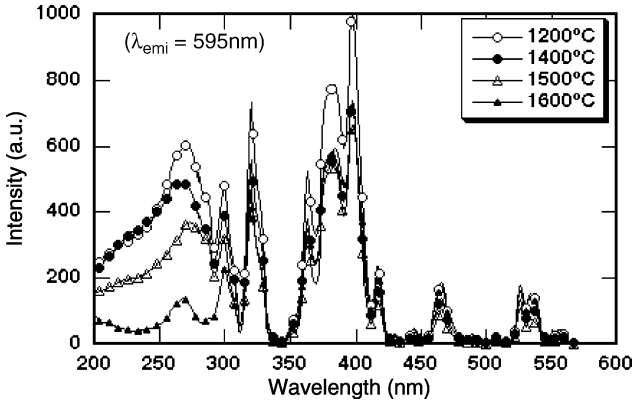

Fig. 7. Room temperature photoluminescence excitation spectra of $EuPO_4$ monitored at 595 nm wavelength, sintering temperatures 1200, 1300, 1400, 1500, and 1600 °C.

powders were cold pressed to form pellets under 200 MPa pressure. Luminescence lifetimes of samples sintered at different temperatures were measured with 0.1 ms delay after the excitation. Data were collected directly in the form of luminescence decay curve from which the lifetime was determined. The excitation wavelength was 396 nm. Measurements were obtained at different emission wavelengths (595, 616 and 700 nm) and an average of the lifetime at a given temperature was taken. Fig. 8 shows an example of the fluorescence decay curves measured. The curves can be well fitted into a single exponential function as $I = I_o \exp(-1/\tau)$ The decay constant obtained was $\tau \sim 0.650 \pm 0.070$ ms.

The measured absorption spectra for samples sintered at 1600 °C is shown in Fig. 9 (sample thickness 0.32 mm), The absorption are due to crystal-field[23] transitions involving deeplying electrons of the Europium. In the ultraviolet range (between 270 and 400 nm) the absorption increases significantly for samples sinterized at higher temperature.

After gamma irradiation of 18 kGy, no changes was observed in the absorption spectrum and overlaps with non irradiated one in the whole wavelength range studied.

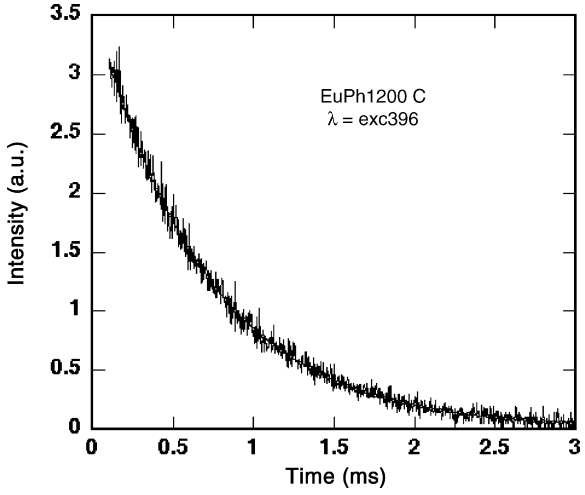

Fig. 8. Fluorescence lifetime of $EuPO_4$ sintered at 1200 °C. The excitation wavelength was 396 nm and monitor wavelength was 595 nm. The smooth line is the exponential fitting function.

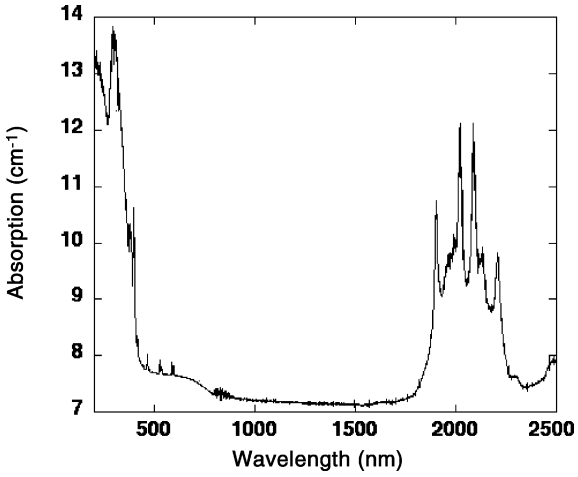

Fig. 9. Absorption spectra for samples sintered at 1600 °C.

4. Conclusions

When the europium phosphate is obtained from aqueous solutions of their salt by precipitation, the precipitate contains defined amount of water that still exists as hydroxyl radicals after sintering at elevated temperatures. The characteristics of the calcined powders and a small proportion of amorphous phase provide the full densification at low temperatures of 1300 °C by promoting the grain boundary diffusion. The glass phase could be formed of high flexibility short chains. The intensity of the excitation peak assigned to charge transfer transition (at 267 nm) decrease significantly with sintering temperature. No appreciable differences in the emission spectra were found excitating from f-f transition (396 nm wavelength) and exciting from charge transfer band (267 nm).

γ-irradiation does not produce any noticeable change in the material at the dose studied.

Acknowledgement

The authors are indebted to Miss Montserrat Martín for her help in these experiments.

References

1. Campbell, J. H. and Suratwala, T. I., Nd-doped phosphate glasses for high-energy/hugh-peak-power lasers. *J. Non-Cryst. Sol.*, 2000, **263**, 318–341.
2. Chen, R. and Lockwood, D. J., Developments in Luminiscence and Display Materials Over the last 100 Years as Reflected in Electrochemical Society Publications. *J. Electrochem. Soc.*, 2002, **149**(9), S69–S78.
3. Ewing, R. C., Nuclear Waste Forms for Actinides. *Proc. Natl. Acad. Sci.*, 1999, **96**, 3432–3439.
4. Assaaoudi, H., Ennaciri, A. and Rulmont, A., Vibrational Spectra of Hydrated Rare Earth Orthophosphates. *Vibrational Spectrosc.*, 2001, **25**, 81–90.
5. Cole, J. M., Van Eck, E. R. H., Mountjoy, G., Anderson, R., Brennan, T., Bushnell-Wye, G., Newport, R. J. and Saunders, G. A., An X-ray Diffraction and 31P MAS NMR Study of rare earth phosphate glasses, $(R_2O_3)x(P_2O_5)_{1-x}$, $x = 0.175$–0.263, R = La, Ce, Pr, Nd, Sm, Eu, Gd, Tb, Dy, Ho. *Er. J. Phys. Condens. Matter.*, 2001, **13**, 4105–4122.
6. Selevich, A. F., Lyakhov, A. S. and Lesnikovich, A. I., Phase equilibrium in the systems Ln_2O_3-P_2O_5-H_2O: regularities of formation and some prop-

erties of rare earth phosphates. *Phosphorous Res. Bull.*, 1999, **10**, 171–176.
7. Guo, Y., Woznicki, P., Barkatt, A., Saad, E. E. and Talmy, I. G., Sol–gel synthesis of microcrystalline rare earth orthophosphates. *J. Mater. Res.*, 1996, **11**(3), 639–649.
8. Hikichi, Y., Synthesis of monazite (RPO_4, R = La, Ce, Nd, or Sm) by sollid state reaction. *Mineralogical J.*, 1991, **15**(6), 268–275.
9. Kijkowska, R. LeGeros, R. Z. Preparation and Properties of Lanthanide Phosphates. *Key. Eng. Mat.*, 2005, **284–286**, 79–82.
10. Terra, O., Clavier, N., Dacheux, N. and Podor, R., Preparation and characterization of lanthanum-gadolinium monazites as ceramics for radioactive waste storage. *New J. Chem.*, 2003, **27**, 957–962.
11. Jonasson, R. G. and Vance, E. R., DTA study of the rhabdiphane to monazite transformation in rare earths (La-Dy) phosphates. *Termochimia Acta.*, 1986, **108**, 65–72.
12. Hirai, H., Masui, T., Imanaka, N. and Adachi, G.-Y., Characterization and thermal behaviour of amorphous rare earth phosphates. *J. Alloys Compounds.*, 2004, **37**, 84–88.
13. Lucas, S., Champiion, E., Bernache-Assollant, D. and Leroy, G., Rare earth phosfate powders $RePO_4.nH_2O$ (Re = La, Ce or Y) part II. Thermal Behaviour. *J. Solid State Chem.*, 2004, **177**, 1312–1320.
14. Lucas, S., Champion, E., Bregiroux, D., Bernache-assollant, D. and Audubert, F., Rare earth phosfate powders $RePO_4{\cdot}nH_2O$ (Re = La, Ce or Y) part I. synthesis and characterization. *J. Solid State Chem.*, 2004, **177**, 1302–1311.
15. Sun, K. and Risen, W. M., Rare earth phosphate glasses. *Solid State Comm.*, 1986, **60**(9), 697–700.
16. Dexpert-Ghys, J., Mauricot, R. and Faucher, M. D., Spectroscopy of Eu^{3+} monazite type lanthanide orthophosphates $LnPO_4$ Ln = La or Eu. *J. Lumin.*, 1996, **69**, 203–215.
17. Blasse, G. and Grabmaier, B. C., *Luminescent Materials*. Springer, Berlin, 1994, p 41.
18. Blasse, G. and Bril, A., Luminescence of phosphoros based on host lattices ABO_4 (A is Sc, In; B is P, V, Nb). *J. Chem. Phys.*, 1969, **50**, 2974–2980.
19. Gonzalez, F., Schabes-Retchkiman, P. and Garcia-Macedo, J., Luminescence of Eu^{3+} incorporated into PZT tetragonal ceramic prepared by Sol-Gel. *J. Phys. D. Appl. Phys.*, 2004, **37**, 2442–2445.
20. Yu, M., Lin, J., Fu, J., Zhang, H. J. and Han, Y. C., Sol–gel synthesis and photoluminescent properties of $LaPO_4$: A (A = Eu^{3+}, Ce^{3+}, Tb^{3+}) nanocrystallyne thin films. *J. Mater Chem.*, 2003, **13**, 1413–1419.
21. Song, H., Lu, S., Shulin, E., Gao, R., Zhang, J., Chen, B., Xia, H., Zhang, Jialin and Ni, Q., Fluorescence properties of divalent and trivalent europium ions in aluminosilicate glasses. *J. Appl. Phys.*, 2002, **91**, 2959–2964.
22. Chen, G., Hölsa, J. and Peterson, J. R., A luminescence study of single-crystal $EuPO_4$ at high pressure. *J. Phys. Chem. Solids.*, 1997, **58**, 2031–2037.
23. Clark, R. N., Chapter 1: Spectroscopy of Rocks and Minerals, and Principles of Spectroscopy. In *Manual of Remote Sensing, Volume 3, Remote Sensing for the Earth Sciences*, ed. A. N. Rencz. John Wiley and Sons, New York, 1999, pp. 3–58.